

Characterizing the effects of fines on the liquefaction resistance of silty sands

Xiao Wei, Jun Yang*

Department of Civil Engineering, The University of Hong Kong, Hong Kong

Received 29 November 2018; received in revised form 18 July 2019; accepted 22 August 2019

Available online 2 November 2019

Abstract

Recent earthquakes in New Zealand and Japan indicate that evaluating the liquefaction potential of silty sands remains an area of difficulty and uncertainty in geotechnical engineering. This paper presents a comprehensive experimental study along with analysis and interpretation in the framework of critical state soil mechanics, with the aim to address the complicated effects of fines. Two series of sand-silt mixtures, formed by mixing two different base sands with the same type of non-plastic silt, were tested under a range of packing density, confining pressure and silt content, and a unified correlation was established between the cyclic resistance and the state parameter that collectively accounts for the effect of packing density and confining pressure. The proposed correlation is independent of packing density, confining pressure, fines content and base sand, and allows prediction of the cyclic resistance of silty sands under different states. Furthermore, the mechanism of the fines-content induced reduction of cyclic resistance and the mechanism of the base-sand effect observed from the tests are elaborated in the sound theoretical context. The present study suggests that the critical state soil mechanics is a rational and appealing framework for liquefaction analysis of both clean and silty sands.

© 2019 Production and hosting by Elsevier B.V. on behalf of The Japanese Geotechnical Society.

Keywords: Silty sand; Critical state soil mechanics; Cyclic resistance; State parameter; Fines content

1. Introduction

1.1. Background

Liquefaction of soils has drawn significant engineering concern ever since the 1964 Niigata earthquake because of disastrous consequences. Extensive investigations have been focused on reconstituted clean sand specimens, yet liquefaction potential of silty sands remains a poorly understood issue even after decades of investigations (e.g. Chang, 1987; Kokusho et al., 2012; Liu and Mitchell, 2006; Papadopoulou and Tika, 2008; Shen et al., 1977;

Stamatopoulos, 2010; Stamatopoulos et al., 2015), as evidenced by damage to lifelines and modern buildings observed in recent earthquakes (Cubrinovski et al., 2011; Yasuda et al., 2012). Since silty sands widely exist in nature and in various engineering projects (e.g. land reclamation and embankments), it is important to carry out research on liquefaction behaviour of silty sands.

1.2. Literature review

Early studies mainly focused on the effects of fines content (FC) on the cyclic behavior and resistance of silty sands (e.g. Carraro et al., 2003; Chien et al., 2002; Dash and Sitharam, 2009; Kuerbis et al., 1988; Xenaki and Athanopoulos, 2003). The cyclic resistance, commonly represented by cyclic resistance ratio (CRR), was found to either increase or decrease with increasing FC , depend-

Peer review under responsibility of The Japanese Geotechnical Society.

* Corresponding author at: Department of Civil Engineering, The University of Hong Kong, Pokfulam, Hong Kong.

E-mail address: junyang@hku.hk (J. Yang).

Nomenclature

List of symbols and abbreviations

<i>CRR</i>	cyclic resistance ratio	K_{fc}	correction factor for fines content
<i>CSL</i>	critical state line	<i>MSF</i>	magnitude scaling factor
<i>CSR</i>	cyclic stress ratio	M_w	moment magnitude
C_u	coefficient of uniformity	N_1	number of cycles to liquefaction/failure
<i>D.A.</i>	double amplitude	p' (p'_c)	mean effective stress (after consolidation)
D_{50}	Mean particle size, i.e. particle size with 50% of particles finer	p'_{cs}	mean effective stress at critical state
<i>Dr</i>	relative density	<i>PSD</i>	particle size distribution
e (e_c)	void ratio (after consolidation)	q_{cyc}	amplitude of cyclic deviatoric stress
e_{cs}	void ratio on the CSL	<i>TSS</i>	toyoura sand + crushed silica silt
e_{eq}	equivalent intergranular void ratio	Δu , <i>EPWP</i>	excess pore water pressure
e_{sk}	Skeleton void ratio	ε_a	axial strain
e_Γ	intercept of CSL in the compression plane	λ_c	gradient of CSL in the compression plane
<i>FC</i>	fines content	σ'_1 (σ'_{1c})	effective axial stress (after consolidation)
FC_{th}	threshold fines content	σ'_3 (σ'_{3c})	effective lateral stress (after consolidation)
<i>FSS</i>	Fujian sand + crushed silica silt	σ'_n (σ'_{nc})	effective normal stress (after consolidation)
		ψ	state parameter

ing on the state variables chosen for comparison, such as void ratio (e) (Dash and Sitharam, 2009; Xenaki and Athanasopoulos, 2003), relative density (Dr) (Carraro et al., 2003; Chien et al., 2002), and skeleton void ratio (e_{sk}) (Carraro et al., 2003; Dash and Sitharam, 2009; Kuerbis et al., 1988). Some researchers also used the equivalent inter-granular void ratio (e_{eq}) to unify the cyclic resistance of sand-fine mixtures (Thevanayagam et al., 2000). Among these state variables, relative density has been commonly adopted as a state variable to characterize the cyclic resistance of clean sands. Yang and Sze (2011b) have shown that the cyclic resistance ratio of clean Toyoura sand and Fujian sand to be close when compared at the same relative density for a given confining pressure and initial static shear stress. However, when relative density is applied to sand-fine mixtures, controversial conclusions may arise. For example, it has been reported that at the same relative density, the cyclic resistance can increase (e.g. Amini and Qi, 2000), decrease (e.g. Chien et al., 2002), first increase then decrease (e.g. Carraro et al., 2003), or remain nearly the same (e.g. Polito, 1999) with increasing fines content up to a threshold value. Such diverse observations are probably due to uncertainties associated with measuring the maximum and minimum void ratios. Yang et al. (2015) presented an investigation into the rationale behind several state variables, including e , e_{sk} and e_{eq} , suggesting that the conventional void ratio remains a proper density index that is particularly suited to the framework of critical state soil mechanics. When compared at the same void ratio, the cyclic resistance of silty sands firstly decreases with increasing fines content until a threshold fine content, FC_{th} , is reached, and then increases with fines content if $FC > FC_{th}$, as shown in Fig. 1(a) for two different sands mixed with the same

non-plastic silt (Polito, 1999). The threshold fines content is a practical boundary separating the sand-dominated and fines-dominated structures, with a typical value of about 30–40%.

Nevertheless, the traditional void-ratio based analysis has several limitations when it is used to characterise the cyclic resistance of sands and silty sands. One of the limitations is that utilisation of void ratio can lead to material-specific correlations, as shown in Fig. 1(b) using the data of Polito (1999). There are two series of test data, the Monterey sand series and the Yatesville sand series. For each series, the FC -specific CRR - e curve shifts to the left with increasing fines content. For a given fines content, different base sands give different trendlines in the CRR - e plane, showing that the base sand properties affect the CRR - e correlations. Such combined effects of fines content and sand properties make it difficult to characterize the cyclic resistance of silty sands. In addition, the cyclic resistance and the mechanical behaviors of silty sands are not only dependent on the void ratio but also on the initial effective stress (e.g. Murthy et al., 2007; Yang and Sze, 2011a, 2011b; Yang and Wei, 2012). This leads to another limitation of the void-ratio based analysis, i.e. the effects of initial effective confining pressure need to be considered separately, as commonly seen in the literature. Apparently, the void-ratio based (and other density-variable based) analysis is not capable of accounting for the combined effects of various factors in a satisfactory way. There is a desire to seek a unified framework of analysis. Since it is widely accepted that the cyclic behaviors of sands and silty sands are dependent on the initial state of the soil, the state parameter (Been and Jefferies, 1985), which was proposed in the framework of critical state soil mechanics (Fig. 2), has received increasing attention in characterising the mechanical behaviors of

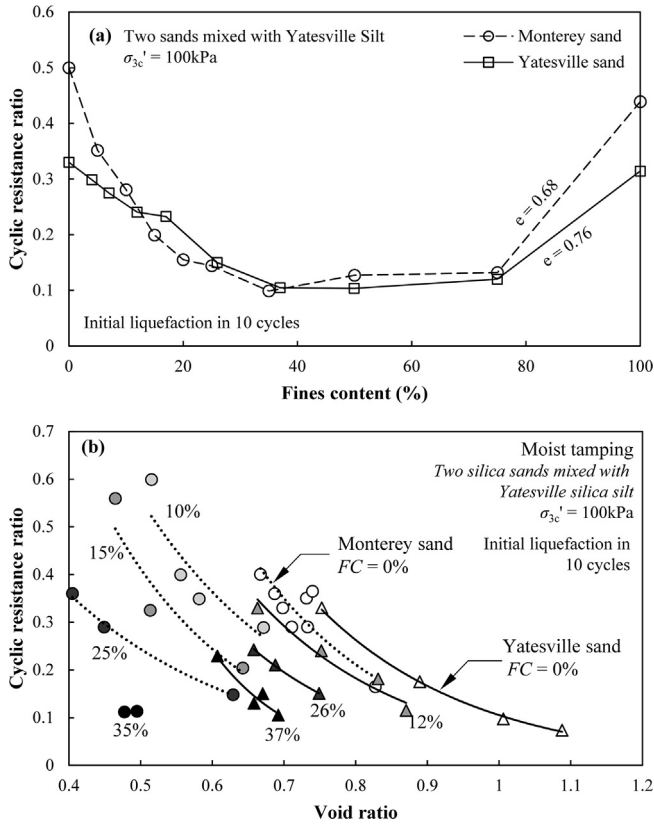


Fig. 1. Cyclic resistance of two silty sands (data from Polito, 1999) (a) Effects of fines on the cyclic resistance of silty sands when compared at the same void ratio; (b) Material specific correlations between cyclic resistance and void ratio.

sands (e.g. Yang, 2002; Yang and Li, 2004) and silty sands (e.g. Murthy et al., 2007; Yang and Wei, 2012; Yang and Liu, 2016), including strength, dilatancy, and small-strain stiffness. The state parameter is also useful to characterize

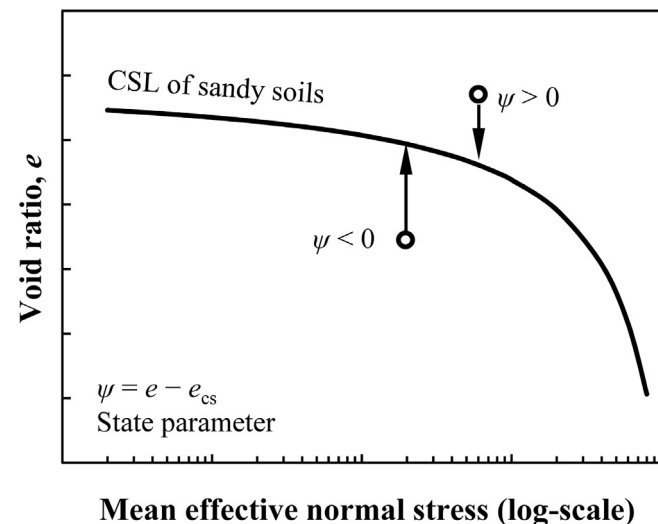


Fig. 2. Schematic definition of the state parameter.

the cyclic resistance of clean sands (Yang and Sze, 2011a, 2011b) and silty sands (Stamatopoulos, 2010; Wei and Yang, 2019). Notably, Yang and Sze (2011a, 2011b) established a state-parameter platform to characterize the cyclic resistance of clean sands considering different initial static shear stresses. Their experimental data show that the cyclic resistance decreases with increasing state parameter for each initial static shear stress level. Wei and Yang (2019) extended this framework to silty sands and showed that the cyclic resistance of sands with different fines contents can be characterised using this platform in a unified way. However, there are no published studies considering the combined effects of fines content and different material properties (such as particle characteristics, gradational properties, etc.) on this promising state-parameter platform.

1.3. Scope of this study

In light of the above, this paper presents a systematic laboratory study aiming to explore the combined effects of fines content and material properties on cyclic resistance of silty sands. Well-controlled cyclic triaxial tests have been conducted on different sand-silt mixtures at different initial states. Besides using the traditional method of analysis, the test results have also been analysed carefully in the framework of critical state soil mechanics. An improved platform is put forward to characterize the cyclic resistance of silty sands with different fines contents and different other properties in a unified way.

2. Testing programme

2.1. Materials

The sand-fine mixtures tested in this study were formed by mixing two different base sands, i.e. Toyoura sand (TS) and Fujian sand (FS), with a non-plastic crushed silica silt. Fig. 3 presents the particle size distribution (PSD) curves of the sands and the silt. The SEM images of the particles are also included. The basic properties of the tested materials are summarized in Table 1. TS is a uniform silica sand with sub-rounded to sub-angular particles and has been widely used in liquefaction research. Fujian sand is a sub-rounded to sub-angular sand with a PSD curve almost parallel to that of TS but with a larger mean particle size (D_{50}). The crushed silica silt was added into Toyoura sand at three fines contents ($FC = 0, 10$ and 20% , denoted by TS, TSS10, TSS20, respectively) to form the sand-silt mixtures referred to as TSS series. Similarly, the silica silt was added into Fujian sand to form the FSS series, i.e. FS and FSS10 for $FC = 0$ and 10% , respectively. The use of artificial mixtures allows good control of grain characteristics and repeatability of the test results and thus eliminates other complex effects or uncertainties.

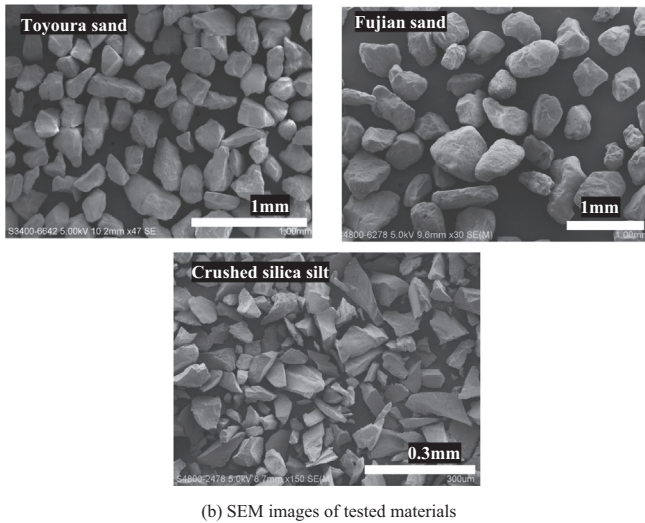
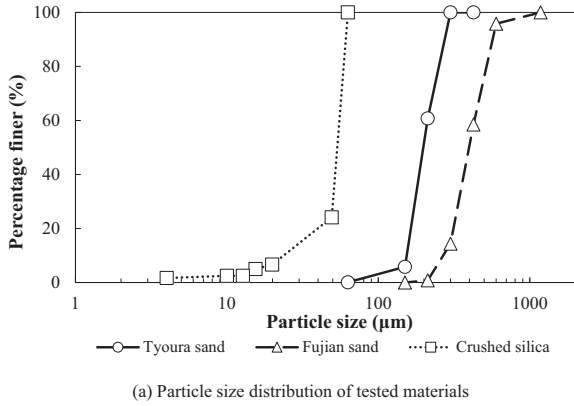


Fig. 3. PSD curves and SEM images of tested materials.

Table 1
Material properties.

Material	D ₅₀ (mm)	C _u	C _c	G _s
Toyouara sand	0.198	1.367	0.962	2.64
Fujian sand	0.397	1.532	0.971	2.65
Crushed silica	0.053	2.182	1.776	2.65

2.2. Test procedures

A series of undrained cyclic triaxial tests was performed under various initial states (in terms of void ratio and mean effective stress, prior to cyclic loading). The specimens were reconstituted by the moist tamping method (MT) in conjunction with the under-compaction technique (Ladd, 1978). Details of the sample preparation method follow those from the investigation by Sze and Yang (2014). All reconstituted specimens were saturated by percolation of CO₂ and de-aired water, and then by applying back pressure. Given that liquefaction resistance is sensitive to the degree of saturation (Yang, 2002b; Yang et al., 2004), the condition of full saturation was considered when the B-

value was greater than 0.98. Then the specimens were isotropically consolidated to the desired effective confining pressure and then loaded under cyclic deviatoric stress cycles. The loading magnitude is represented by the cyclic stress ratio, CSR, which is defined by the following equation,

$$CSR = \frac{q_{cyc}}{2\sigma'_{nc}} = \frac{q_{cyc}}{\sigma'_{1c} + \sigma'_{3c}} \quad (1)$$

where q_{cyc} is the amplitude of the cyclic deviatoric stress; σ'_{nc} is the normal effective stress on the maximum shear stress plane; σ'_{1c} and σ'_{3c} are the axial and lateral effective stress after consolidation, respectively. For isotropically consolidated specimens, σ'_{nc} is equal to p'_c (the mean effective stress after consolidation). The initial void ratio prior to cyclic loading or the post-consolidation void ratio (e_c) was carefully determined by measuring the water content after testing (Yang and Wei, 2012). This is because the post-consolidation void ratio can be deemed to equal to the void ratio after test, due to the undrained shearing condition.

The experiments in the study covered a reasonably wide range of states in terms of density, confining stress and fines content. The wide range allows the development of a better understanding in the context of critical state soil mechanics, as described in later sections. Table 2 summarizes the testing conditions and corresponding initial state parameters for different specimens, as well as the measured CRR values. The critical state line (CSL) data were extracted from Liang (2016) for TSS10 and TSS20 and from Yang and Wei (2012) for FSS10. The following formulation was used to depict the non-linearity of the CSL in the e -log p' plane (Li and Wang, 1998; Yang and Li, 2004).

$$e_{cs} = e_{\Gamma} - \lambda_c \left(\frac{p'_{cs}}{p_a} \right)^{\xi} \quad (2)$$

where e_{cs} and p_{cs}' represent the loci of CSL; e_{Γ} and λ_c are the intercept and the slope of CSL in the e - $(p_{cs}'/p_a)^{\xi}$ plane, respectively.

3. Failure patterns

Three typical failure patterns were observed in the tested specimens, i.e. flow failure, cyclic mobility, and limited flow, which were also observed on clean sands (Sze and Yang, 2014) and natural sandy soils (Wei et al., 2018).

3.1. Flow failure

Flow failure is a failure pattern characterised by the sudden and rapid development of strain without significant pre-failure strain accumulation (pre-failure e_a with a single amplitude <5%). Fig. 4a presents typical test results from a moist-tamped TSS10 specimen exhibiting flow failure. The stress-strain relationship shows that the axial strain is not obvious before its sudden and rapid development on the

Table 2
Summary of test results.

Material*	SPM	e_c^{**}	p'_c (kPa)	ψ	CRR_{10}	CRR_{15}	CRR_{20}	Failure pattern
TSS10	MT	0.906	100	0.030	0.148	0.141	0.136	Flow
		0.903	300	0.060	0.118	0.111	0.107	Flow
		0.849	100	−0.027	0.179	0.173	0.168	Limt. Flow
		0.791	40	−0.100	0.323	0.291	0.270	Cyclic mob.
		0.795	100	−0.081	0.269	0.248	0.235	Cyclic mob.
		0.794	300	−0.049	0.205	0.193	0.185	Cyclic mob.
		0.722	100	−0.154	0.422	0.378	0.350	Cyclic mob.
TSS20	MT	0.916	100	0.089	0.080	0.073	0.069	Flow
		0.905	100	0.078	0.110	0.104	0.101	Flow
		0.790	40	−0.053	0.240	0.227	0.218	Cyclic mob.
		0.795	100	−0.032	0.204	0.190	0.181	Cyclic mob.
		0.794	300	0.003	0.162	0.152	0.146	Flow
		0.719	100	−0.108	0.311	0.284	0.267	Cyclic mob.
FSS10	MT	0.813	100	0.075	0.110	0.102	0.097	Flow
		0.717	100	−0.021	0.191	0.179	0.171	Cyclic mob.

* The critical state lines are from Liang (2016) for TSS10 and TSS20 and from Yang and Wei (2012) for FSS10.

** Average void ratio after consolidation.

extension side (negative ϵ_a). Once flow failure is triggered, the axial strain may develop quickly to the limit of the apparatus (single amplitude $\epsilon_a > 20\%$) within a very short period of time. The excess pore water pressure (EPWP) increases cyclically due to each cycle of loading before failure, and then increases suddenly to reach a value equal to the initial confining pressure. The stress path also indicates that the effective stress of the specimen decreases progressively in each cycle and then suddenly dropped to zero, indicating that the specimens completely liquefied after flow failure. This type of failure is associated with sudden and unlimited flow in newly and loosely deposited natural and artificial soils.

3.2. Cyclic mobility

Cyclic mobility (Castro, 1975) describes the behavior where the specimen undergoes a transient liquefied state ($\Delta u = \sigma'_{nc}$, $p' = 0$ or $\sigma'_n = 0$) upon the reversal of cyclic loading. Fig. 4b presents typical cyclic mobility using test results from a moist-tamped TSS10 specimen. The excess pore water pressure increases cyclically and the soil finally reaches the transient liquefied state. When this state is reached for the first time, initial liquefaction occurs, and significant axial strain development can take place during subsequent cyclic loading. These transient liquefied states correspond to reversal of the deviatoric stress direction, either from compression to extension or from extension to compression. Large axial strain development can take place when the load is about to reverse its direction and the specimen exhibits very low stiffness because of low effective stress. After the loading direction reverses, stiffness and strength of the specimens can recover with further loading, corresponding to a decrease in pore water pressure and an increase in effective stress.

3.3. Limited flow

Limited flow is a failure pattern that may include some features of both flow failure and cyclic mobility. Fig. 4c presents typical test results from moist-tamped TSS10 specimens exhibiting limited flow. The axial strain suddenly increases without significant pre-failure accumulation but ceases before exceeding the limit of the apparatus. The axial strain development during limited flow is about 10% (single amplitude) on the extension side. The excess pore water pressure increases progressively during each cycle, whereas the effective stress decreases before flowing. During limited flow, the increase of excess pore water pressure, or decrease of effective stress is approximately 20 kPa. However, the subsequent unloading can induce a dramatic increase in pore pressure and a decrease in effective stress, leading to a completely liquefied state ($\Delta u = \sigma'_{nc}$, $p' = 0$ or $\sigma'_n = 0$). This liquefied state seems to be transient for the specimen, because the pore pressure started to reduce and effective stress to increase upon reversal of loading direction. However, the specimen failed to regain its strength because significant axial strain took place, shortly after the transient liquefied state, and thus leading to termination of the test. Similar to the flow failure mentioned previously, this type of failure also leads to rapid failure without sufficient warning. The magnitude of flow seems to be dependent on both the state of the soil and the amplitude of cyclic loading.

4. Cyclic resistance of silty sands

4.1. Determination of cyclic resistance

For specimens exhibiting flow-type failure (i.e. flow failure and limited flow), the onset of flow is defined as failure

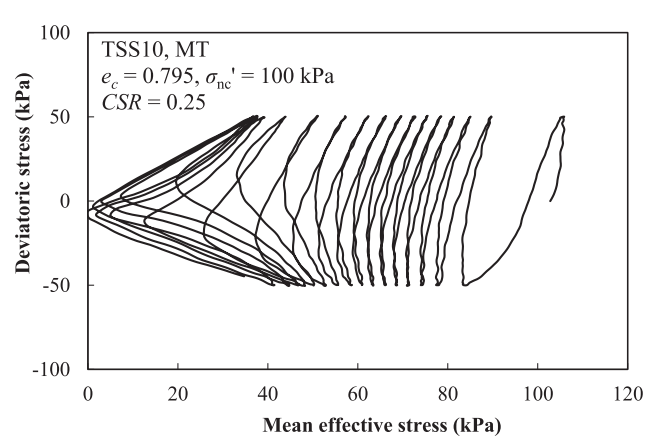
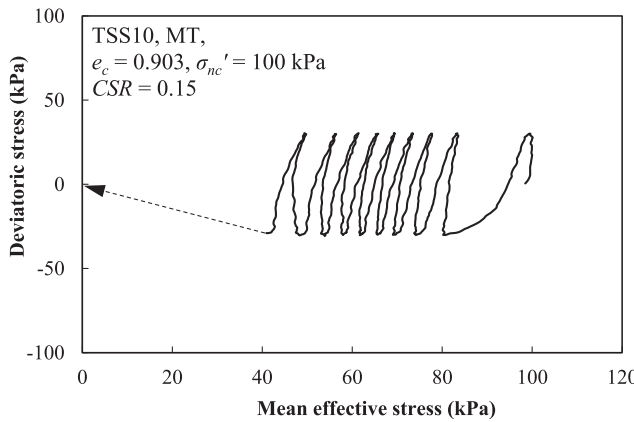
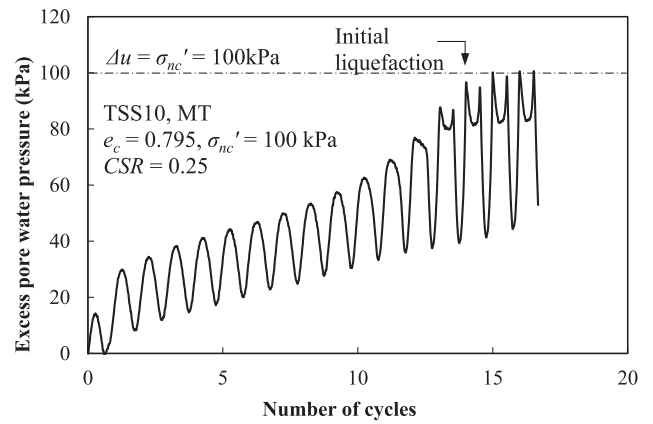
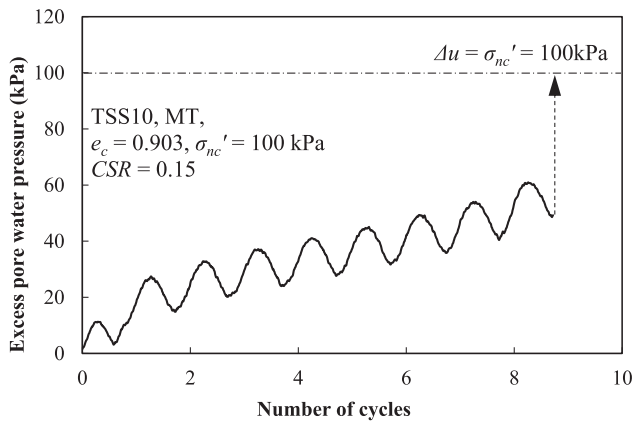
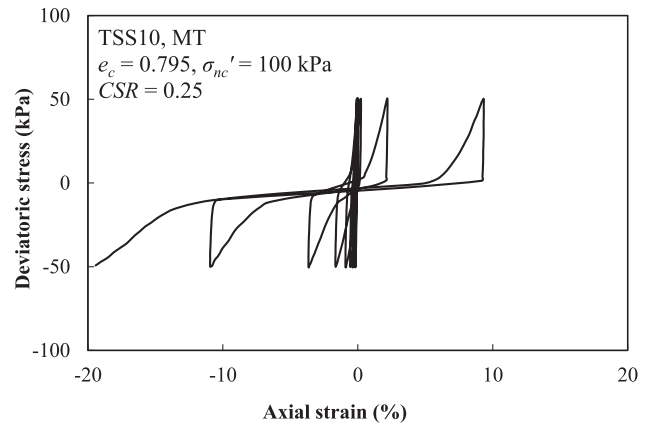
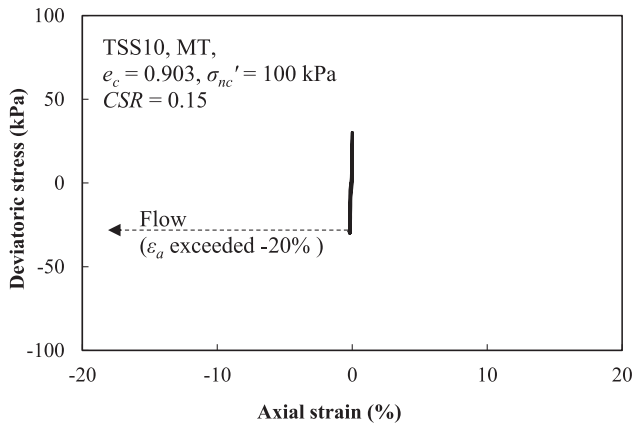


Fig. 4a. Flow failure (TSS10, $e_c = 0.903$, $\sigma_{nc}' = 100$ kPa, $CSR = 0.15$, MT).

Fig. 4b. Cyclic mobility (TSS10, $e_c = 0.795$, $\sigma_{nc}' = 100$ kPa, $CSR = 0.25$, MT).

(at this moment the axial strain usually develops rapidly to a level much larger than 5%). Whereas for specimens exhibiting cyclic mobility, failure is defined by attaining 5% double amplitude (D.A.) of axial strain.

Different CSR s were applied to replicated specimens and thus caused different numbers of cycles to failure/liquefaction (N_f). Typical $CSR-N_f$ relationships are presented in Fig. 5 showing that N_f increases with decreasing CSR in a typical power relation (Eq. (3)).

$$CSR = a(N_f)^b \quad (3)$$

The cyclic resistance ratio, CRR , is defined as the CSR causing liquefaction in a given number of cycles (e.g. $N_f = 10$ or 15), corresponding to the moment magnitude (M_w) of an earthquake. According to Idriss (1999), the mean number of equivalent uniform cycles is 10 and 15 for an earthquake with $M_w = 7$ and 7.5 , respectively. Table 2 summarizes the test results including state parameter and CRR values for $N_f = 10, 15$ and 20 .

Values of the normalized cyclic stress ratio (CSR / CRR_{15}) of TSS10 are plotted in Fig. 6(a), showing a unique relationship with $b = 0.135$ regardless of different void

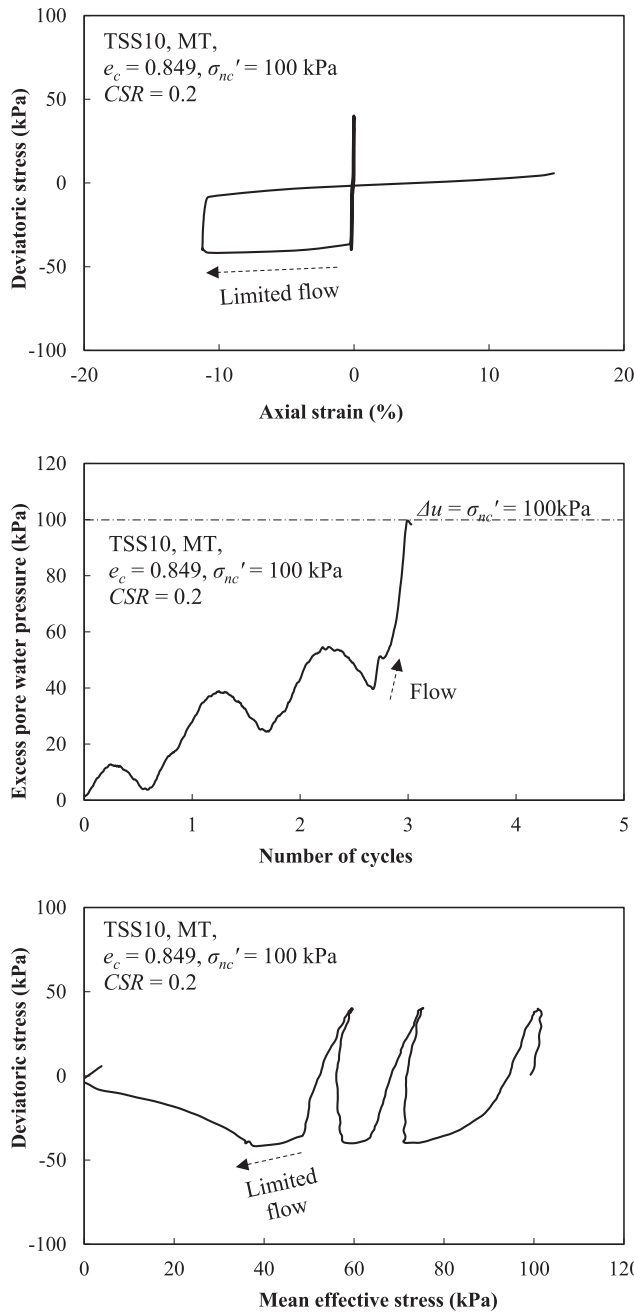


Fig. 4c. Limited flow (TSS10, $e_c = 0.849$, $\sigma'_{nc} = 100$ kPa, $CSR = 0.2$, MT).

ratios and confining stresses. The unique relationship still exists, when the data of clean Toyoura sand and TSS20 are added (Fig. 6(b)). A unique trendline can be found with $b = 0.132$, which is very close to that for TSS10. To compare different series of sand-fine mixtures, the data of FSS series are plotted together with the data of the TSS series in Fig. 6(c). Interestingly, there seems no significant difference between the two series. The b value for the entire data set of TSS and FSS is 0.138. The differences among the three fitted b values are so small that the trendlines cannot be clearly differentiated once they are plotted together. It may be concluded that a unique relationship between the

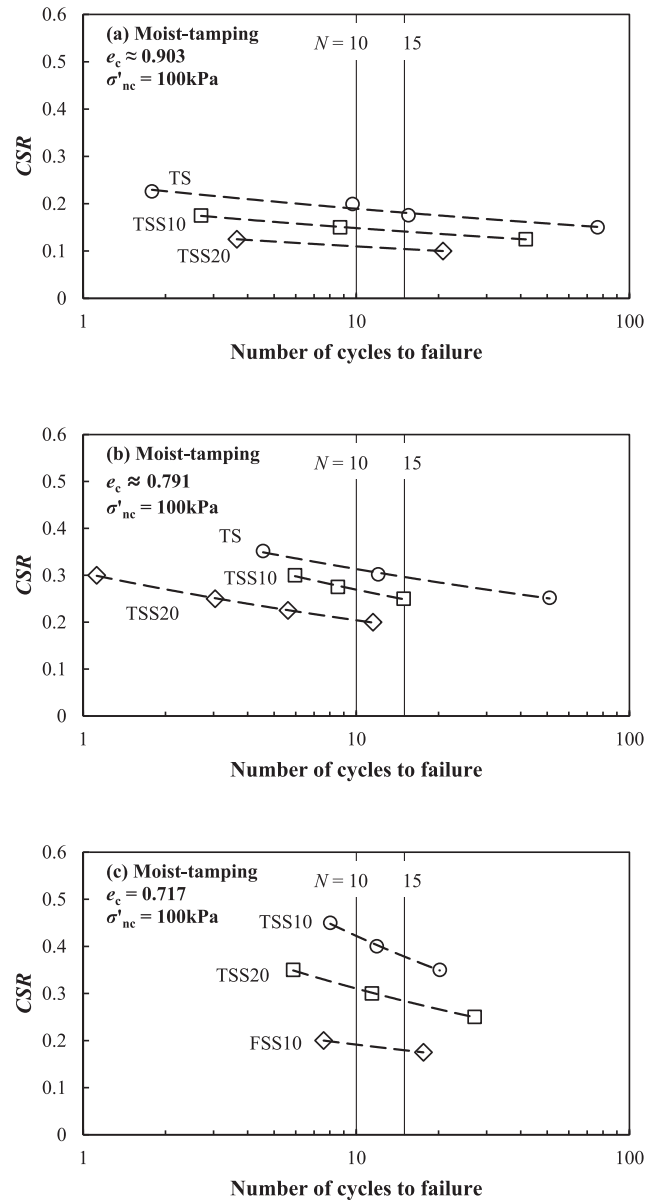


Fig. 5. Typical $CSR-N_1$ relationships of the sand-fines mixtures.

normalized cyclic stress ratio and the number of cycles to liquefaction, regardless of void ratio, confining pressure, fines content and base sand type. It is worth mentioning that this finding differs from that of Boulanger and Idriss (2015), who suggested void ratio-dependent b values. This difference highlights the advantage and rationale of using normalized cyclic stress ratio in the interpretation.

This relationship may be further developed to the relationship between the magnitude scaling factor (MSF) and the moment magnitude (M_w) of an earthquake, as shown in Fig. 7, by assuming CSR equals CRR_N (CRR defined by $CSR-N_1$ relationship at a certain N value) and relating N_1 to M_w according to the suggestion of Idriss (1999). A series of magnitude scaling factors is proposed based on the data of TSS series and compared with several typical

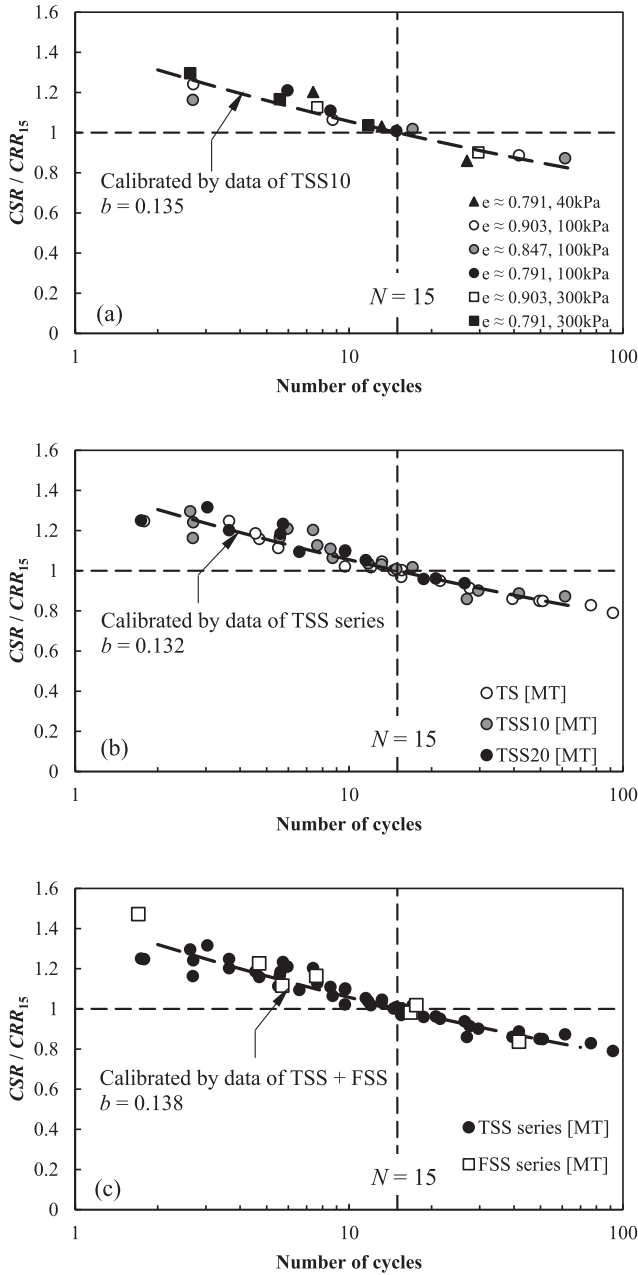


Fig. 6. Unified relationship between N_1 and normalized cyclic stress ratio (a) TSS10, (b) TSS series, (c) TSS and FSS series.

MSF proposals summarized by NCEER committee (Youd et al., 2001). The series of magnitude scaling factors derived from TSS series are very close to those suggested by Seed and Idriss (1982), noting that their proposal is also based on laboratory investigation. However, other researchers have suggested diverse MSF which shows poor consistency. Youd et al. (2001) have recommended the shaded area to be used for engineering practice when $M_w < 7.5$ and the values suggested by Idriss (1999) to be used for $M_w > 7.5$. It seems that the discrepancy between these proposals is not fully understood. The present study suggests that the original MSF suggested by Seed and Idriss

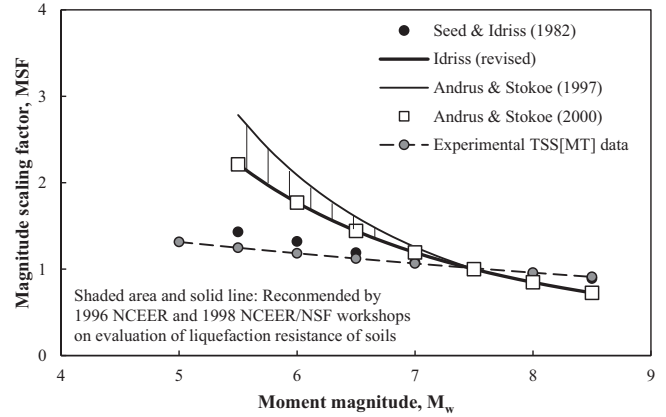
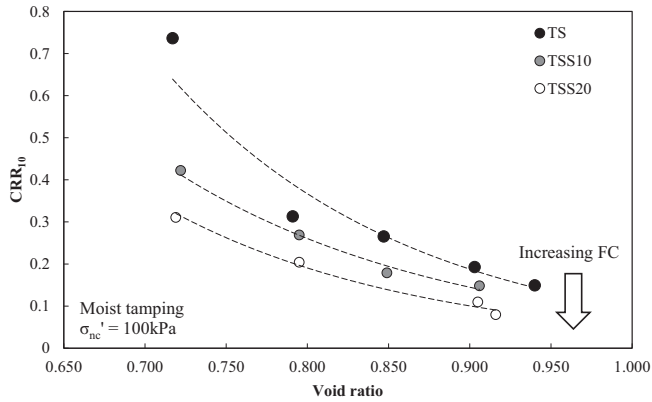


Fig. 7. Comparison between the MSF calibrated by data of TSS series and the existing proposals.

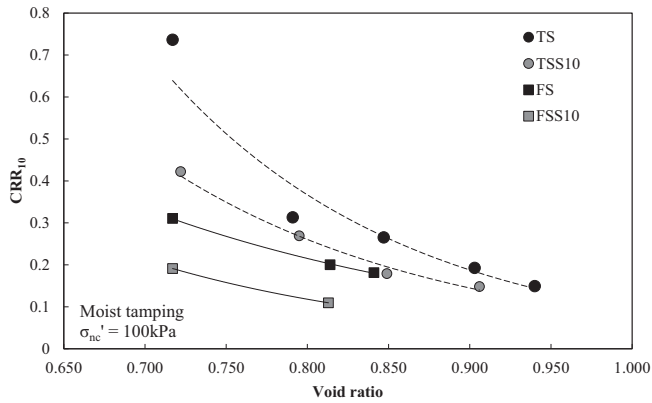
(1982) may be applied to non-plastic reconstituted specimens, regardless of packing density, confining pressure, fines content and soil type. When CRR_{10} or CRR_{15} (commonly determined in laboratory) of a reconstituted sample is obtained by lab testing, one may apply the M_w-N_1 relation proposed by Idriss (1999) and the MSF- M_w relation, either the proposed one or the proposal of Seed and Idriss (1982), to turn the CRR_{10} or CRR_{15} to a cyclic resistance ratio under a certain magnitude of earthquake.

4.2. $CRR-e$ relationships

The CRR of the tested materials decreases with increasing void ratio (Fig. 8). The test results of TSS series are presented in Fig. 8(a), showing a downward shift of the FC -specific $CRR-e$ relationships. The FC -specific relationships indicate that the CRR decreases with increasing FC when compared at the same void ratio. The test results of FSS series are compared with TSS series ($FC = 0$ and 10%) in Fig. 8(b). When compared at the same void ratio and otherwise similar conditions, the CRR values of the FSS series are lower than that of the TSS specimens. The different series occupy distinctly different zones in the $CRR-e$ plane, verifying a material-specific characteristic when the comparison is made at the same void ratio. Other than the fines content, factors affecting the $CRR-e$ relationships of the two series can be the particle shape, the particle size disparity, the gradation of base sands, etc. The effects of these factors interact with each other making the traditional packing-density based (e.g. void-ratio based) characterisation of CRR very complicated. On the other hand, CRR decreases with increasing confining pressure (Fig. 9). The pressure dependency introduces an additional variable and further increases the complexity in characterising the cyclic resistance. Note that CRR_{10} is used here for the analysis, because results for TS and FS are from the previous studies of Yang and Sze (2011a, 2011b) in which only data on CRR_{10} are available. However, the use of



(a) FC-specific CRR - e relationships of the TSS series



(b) Material-specific CRR - e relationships of the TSS and the FSS series

Fig. 8. FC-specific and material-specific CRR - e relationships (clean sand data from Yang and Sze, 2011a, 2011b).

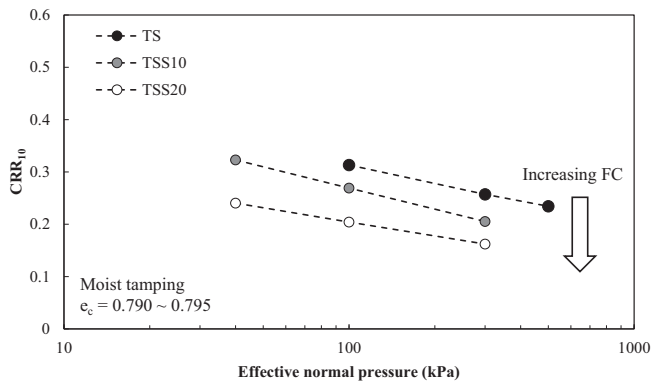


Fig. 9. Effects of the initial confining stress on CRR (clean sand data from Yang and Sze, 2011a, 2011b).

either CRR_{10} or CRR_{15} would not alter the trends presented. For reference, values of CRR_{15} and CRR_{20} derived from the present study are provided.

4.3. Effects of fines content on CRR

The effect of fines content is obvious that CRR decreases with increasing fines content when compared at the same void ratio and other similar conditions (Fig. 10), for both

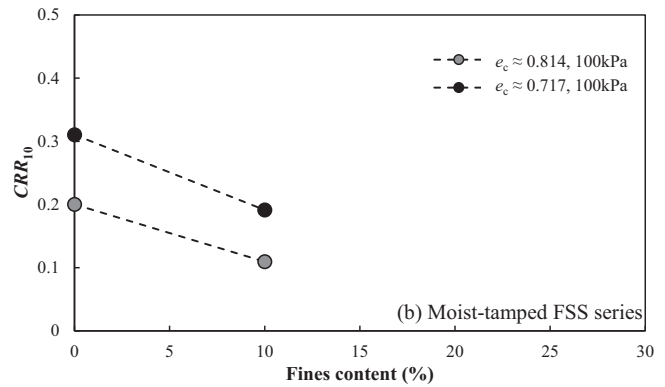
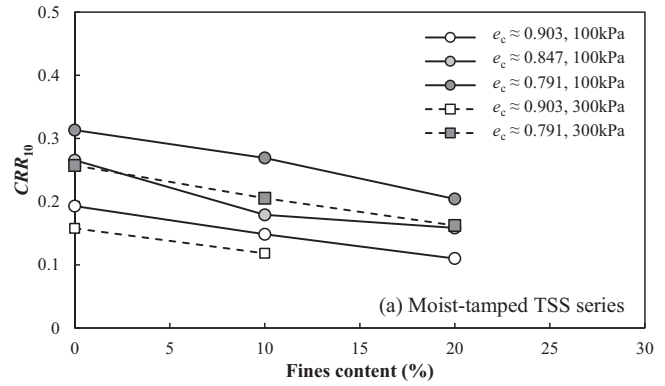


Fig. 10. Effects of fines content on the cyclic resistance.

TSS series and FSS series. Some researchers (Bouckovalas et al., 2003; Polito and Martin, 2003) used a normalized factor (K_{fc}) to characterize the effects of fines on the cyclic resistance, which is defined as follows

$$K_{fc} = \frac{CRR_{fc \neq 0}}{CRR_{fc = 0}} \quad (4)$$

where $CRR_{fc \neq 0}$ and $CRR_{fc = 0}$ are CRR when $FC \neq$ and $= 0$, respectively. This correction factor is applicable only when both the clean sand and the sand-silt mixture are compared under the same initial void ratio and effective confining pressure. The K_{fc} - FC data are presented in Fig. 11 for both TSS series and FSS series showing that K_{fc} decreases with increasing FC . There is a data point of the TSS series (Fig. 11(a)), representing the state of $e_c \approx 0.847$ and $\sigma'_{nc} = 100$ kPa at $FC = 10\%$, is lower than the others. This is probably because of the uncertainties caused by different test operators. If ignore this point, the other data points form a relatively narrow band, giving an average $K_{fc} \approx 0.8$ when $FC = 10\%$, and average $K_{fc} \approx 0.6$ for $FC = 20\%$. It seems that the void ratio and the confining stress do not affect the K_{fc} - FC relationships.

In comparison, the FSS series gives an average $K_{fc} \approx 0.6$ (Fig. 11(b)), which is significantly lower than the TSS series compared at the same FC . This means that the addition of crushed silica fines into Fujian sand leads to a more significant decrease in CRR than the addition into Toyoura sand, noting that the difference between the two series should not be attributed to the uncertainties of the test

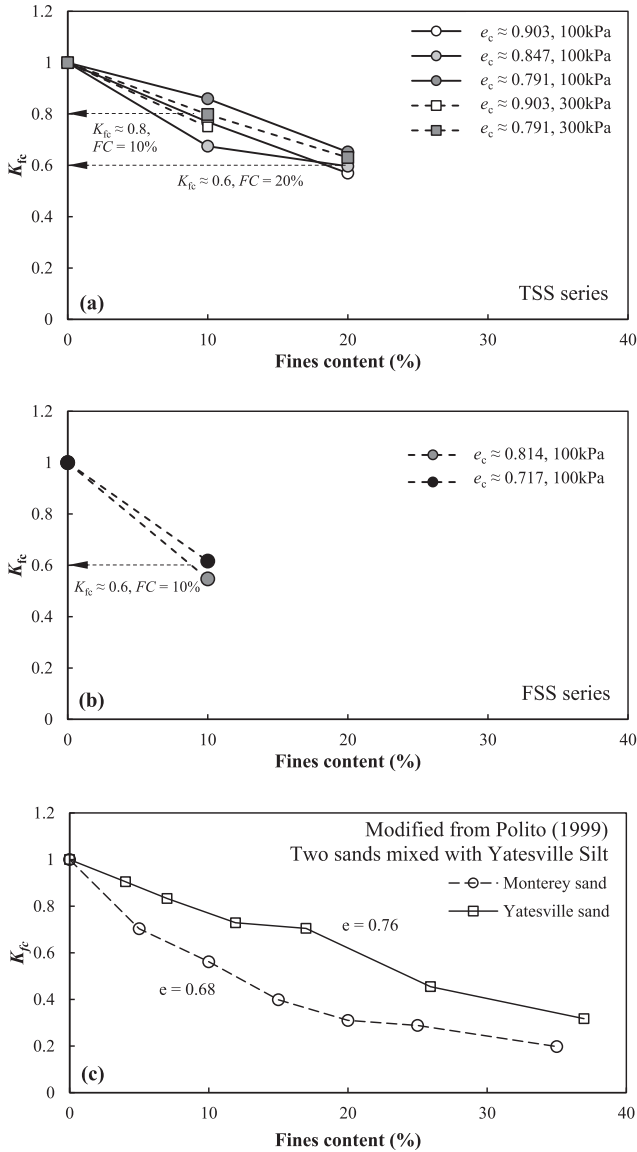


Fig. 11. Reduction of cyclic resistance due to addition of fines.

results. Because even the scatter of the TSS series cannot cover such a huge difference. The difference between the TSS series and the FSS series indicates that the negative effect of fines may be affected by the base sand. Polito (1999) also tested two series of sand-fine mixtures, using different base sands and the same fines. The test results show two different K_{fc} - FC relationships for the two series (Fig. 11(c)). It seems that there are no effective methods to characterize such effects of the base sands in the literature.

5. Critical state-based interpretation

5.1. Unified characterization of CRR

The state parameter, which represents the initial state of sands, can characterize the effects of packing density and

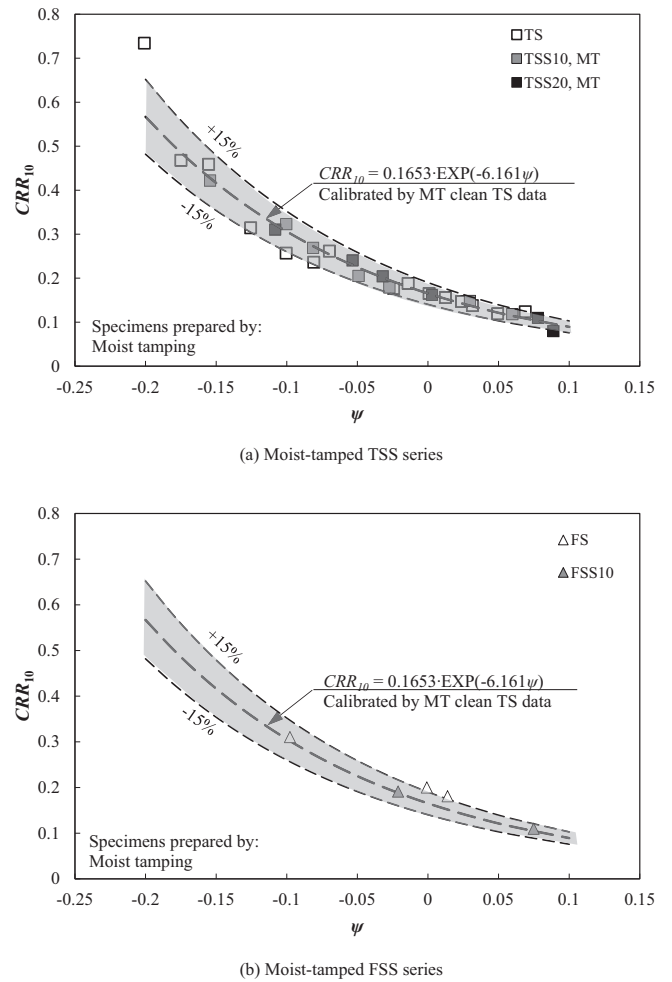


Fig. 12. Unified CRR - ψ correlation.

confining pressure in a unified way. Fig. 12(a) presents the silty sand data in comparison with the trendline calibrated from clean Toyoura sand (Yang and Sze, 2011a). The silty sand data fall into the vicinity of the clean sand trendline. And the trendline seems to be the average line of the silty sand data. The following equation characterizes the best-fitted trendline of the moist-tamped clean Toyoura sand.

$$CRR_{10} = 0.165 \exp(-6.161\psi) \quad (5)$$

Similarly, Stamatopoulos (2010); Papadopoulou and Tika (2008) also suggested almost unified correlations for non-plastic sands with different fines contents. Different from those previous investigations, the present study used different base sands, and thus it is of interest to see whether the unified CRR - ψ correlation derived from TSS series remains suitable for the FSS series. In Fig. 12(b), the data from FSS series also fall into the vicinity of the TSS trendline, indicating a unified correlation for the two series of sand-fine mixtures.

Fig. 13 compares the measured and the predicted CRR values of TSS series and FSS series using Eq. (5) which is

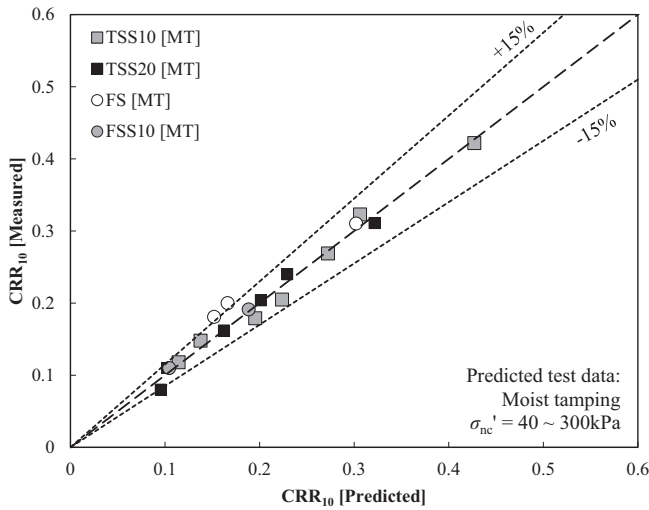


Fig. 13. Validation of the $CRR-\psi$ correlation calibrated from clean TS data.

best-fitted by clean TS data only, noting that the initial state parameters were obtained with reference to the critical state lines reported by Liang (2016); Sze (2010); Wei (2012). The fairly good prediction indicates that the CRR of different non-plastic silica materials may be predicted using a unified $CRR-\psi$ correlation if the specimens are prepared by the moist tamping method. In addition, Wei et al. (2017) also found that the same trendline is applicable to clean sands with different particle shape, indicating that this unified $CRR-\psi$ correlation may have much broader application.

5.2. Effects of FC on CRR

Using Eq. (5), the following derivation becomes straightforward.

$$K_{fc} = \frac{CRR_{fc \neq 0}}{CRR_{fc=0}} = \frac{CRR_{\psi_1}}{CRR_{\psi_2}} = \frac{m \cdot \exp(-n\psi_1)}{m \cdot \exp(-n\psi_2)} = \exp(-n \cdot \Delta\psi) \quad (6)$$

where $m = 0.165$ and $n = 6.161$ for moist-tamped non-plastic siliceous sands and silty sands. By using the critical state lines extracted from Liang (2016); Sze (2010); Wei (2012), the $K_{fc}-FC$ relationships can be predicted using Eq. (6), as shown in Fig. 14. The measured data are also compared with the predicted ones in Fig. 14, showing that the predicted curves capture the general trend of the $K_{fc}-FC$ relationships and provide acceptable estimations of K_{fc} .

Moreover, Eq. (6) clearly indicates that the correction factor is affected by the change of state parameter. And the change of state parameter is due to the effects of fines content on the critical state line. Yang and Wei (2012) and Liang (2016) presented that an addition of non-plastic silts would result in a decrease of e_{Γ} when $FC < FC_{th}$ (Fig. 15). Therefore, when compared at the same initial void ratio and effective confining pressure,

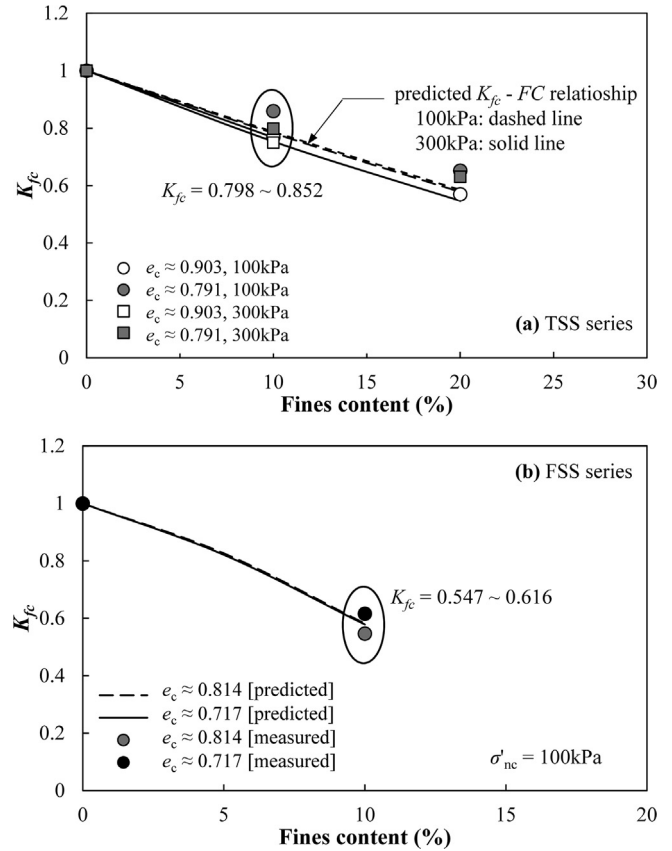


Fig. 14. Effects of fines predicted by the proposed $K_{fc}-FC$ relationship.

addition of non-plastic silts leads to increased state parameter ($\Delta\psi > 0$), causing $K_{fc} < 1$ (i.e. $CRR_{fc \neq 0} < CRR_{fc=0}$).

When $FC > FC_{th}$, several investigations provided evidence that further addition of non-plastic fines would lead to an upward shift of CSL, such as Thevanayagam et al. (2002); Papadopoulou and Tika (2008). Although the critical state framework may be applied in this case, the investigations on higher fines contents seem to be limited. Further study may be needed for $FC > FC_{th}$.

5.3. Effects of base sands

5.3.1. Effects of base sands on CRR

As demonstrated in Fig. 8(b), FS has lower CRR than that of TS when compared at the same initial void ratio and otherwise similar conditions. According to the unified $CRR-\psi$ correlation for both moist-tamped TS and FS, the difference between the CRR s of the two sands can be due to the difference between the initial state parameter of the two sands. Yang and Wei (2012) reported the CSLs of the FSS series are lower than that of the TSS series (Fig. 15). When compared at the same initial void ratio and initial effective confining pressure, the FS specimen has larger ψ than the TS specimen. The larger ψ leads to a lower CRR for the FS specimen, because the CRR decreases with increasing ψ . Similarly, the lower CSL of the FSS10 compared with that of the TSS10 (Fig. 15) leads

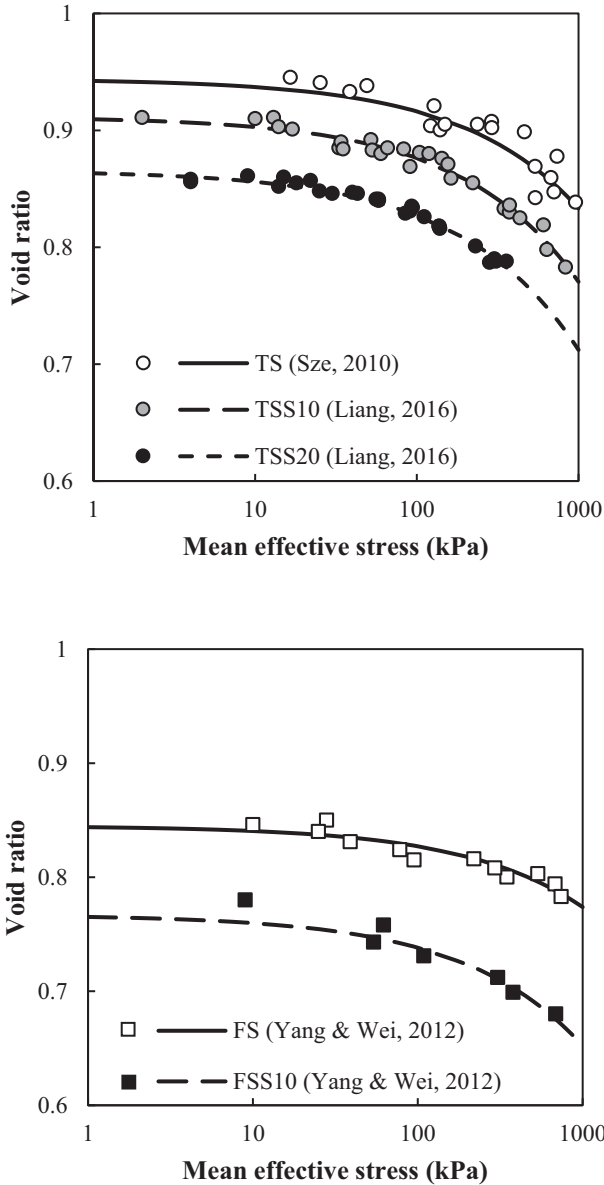


Fig. 15. The CSLs of the TSS series and FSS series.

to lower CRR value of the FSS10 than the TSS10, when the CRR values are compared at the same initial void ratio and effective confining pressure.

5.3.2. Effects of base sand on K_{fc}

The correction factor K_{fc} of FSS10 ($K_{fc} = 0.547 \sim 0.616$) is lower than that of TSS10 ($K_{fc} = 0.798 \sim 0.852$), as shown in Fig. 14. Because K_{fc} is not significantly affected by initial void ratio and effective confining pressure, such difference should be mainly caused by the different properties of the two base sands. According to Eq. (6), the K_{fc} factor is affected primarily by the change of initial state parameter ($\Delta\psi$) with respect to the clean sand, due to the addition of fines. Apparently, the vertical distance between CSLs of FS and FSS10 is larger than that between CSLs of TS and TSS10, as shown in Fig. 15. Namely, $\Delta\psi$ of the FSS series due to addition of fines can be higher than that of

the TSS series. According to Eq. (6), the K_{fc} is thus smaller for the FSS10 than for the TSS10, representing a more significant decrease of CRR due to addition of fines. The distance between CSLs of the base sand and the silty sands is controlled by several factors such as the particle size disparity and the combined shape effects of coarse and fine particles (Yang and Wei, 2012). The effects of these factors may be complex and require further investigation.

6. Conclusion

This paper presents a systematic experimental study aimed at investigating the liquefaction behavior and cyclic resistance of silty sands in the framework of critical state soil mechanics. The major conclusions are summarized as follows.

1. The number of cycles to failure increases with decreasing cyclic stress ratio. When the cyclic stress ratio is normalized by the cyclic resistance, a unified correlation exists between the normalized cyclic stress ratio and the number of cycles to failure, irrespective of packing density, confining pressure, fines content and base sand.
2. The liquefaction resistance of the tested silty sands decreases with increasing fines content when compared at the same void ratio, for $FC < FC_{th}$. A unified $CRR-\psi$ correlation can be established which is irrespective of packing density, confining pressure, fines content and base sand. This correlation is within the framework of CSSM and can be applied to predict liquefaction resistance of both clean sand and silty sands.
3. In the framework of CSSM, the fines-content induced reduction of CRR is attributed to the downward shift of the CSL with the addition of non-plastic fines ($FC < FC_{th}$). This shift results in an increased ψ when compared at the same initial void ratio and at otherwise similar conditions.
4. Similarly, for different types of sand-silt mixtures with similar mineralogy (e.g. TS series and FS series) and the same FC and tested under the same void ratio and effective confining pressure, the different CRR can be attributed to different ψ caused by the different positions of the CSL.
5. The correction factor K_{fc} may reflect the amount of variation of CRR due to change of FC . It is little affected by initial void ratio and effective confining pressure. However, the base sand can affect the $K_{fc}-FC$ relationship for different sand-fine mixtures. The CSSM framework allows a reasonable prediction of the $K_{fc}-FC$ relationship and a sound explanation for the mechanism of the base-sand effects.

Acknowledgement

The financial support provided by the Research Grants Council of Hong Kong (No. 17250316; 17206418) is grate-

fully acknowledged. The research in the early stage also received support from The University of Hong Kong through the Seed Fund for Basic Research scheme.

References

- Amini, F., Qi, G.Z., 2000. Liquefaction testing of stratified silty sands. *J. Geotech. Geoenviron. Eng.* 126 (3), 208–217.
- Been, K., Jefferies, M.G., 1985. A state parameter for sands. *Géotechnique* 35 (2), 99–112.
- Bouckovalas, G.D., Andrianopoulos, K.I., Papadimitriou, A.G., 2003. A critical state interpretation for the cyclic liquefaction resistance of silty sands. *Soil Dyn. Earthq. Eng.* 23 (2), 115–125.
- Boulanger, R.W., Idriss, I.M., 2015. Magnitude scaling factors in liquefaction triggering procedures. *Soil Dynamics Earthquake Eng.* 79, 296–303.
- Carraro, J.A.H., Bandini, P., Salgado, R., 2003. Liquefaction resistance of clean and nonplastic silty sands based on cone penetration resistance. *J. Geotech. Geoenviron. Eng.* 129 (11), 965–976.
- Castro, G., 1975. Liquefaction and cyclic mobility of saturated sands. *J. Geotech. Eng. Div.* 101 (6), 551–569.
- Chang, N.-Y., 1987. Liquefaction Susceptibility of Fine-Grained Soils, Preliminary Study Report. US Army Corps of Engineers.
- Chien, L.-K., Oh, Y.-N., Chang, C.-H., 2002. Effects of fines content on liquefaction strength and dynamic settlement of reclaimed soil. *Can. Geotech. J.* 39 (1), 254–265.
- Cubrinovski, M., Bray, J.D., Taylor, M., Giorgini, S., Bradley, B., Wotherspoon, L., Zupan, J., 2011. Soil liquefaction effects in the central business district during the February 2011 Christchurch earthquake. *Seismol. Res. Lett.* 82 (6), 893–904.
- Dash, H.K., Sitharam, T.G., 2009. Undrained cyclic pore pressure response of sand–silt mixtures: effect of nonplastic fines and other parameters. *Geotech. Geol. Eng.* 27 (4), 501–517.
- Idriss, I.M., 1999. An update to the Seed-Idriss simplified procedure for evaluating liquefaction potential. TRB Workshop on New Approaches to Liquefaction.
- Kokusho, T., Ito, F., Nagao, Y., Green, A., 2012. Influence of non/low-plastic fines and associated aging effects on liquefaction resistance. *J. Geotech. Geoenviron. Eng.* 138 (6), 747–756.
- Kuerbis, R.H., Nigussey, D., Vaid, Y.P., 1988. Effect of gradation and fines content on the undrained response of sand. In: *A Spec. Conf. Hydraul. Fill Struct.* Colorado, USA.
- Ladd, R., 1978. Preparing test specimens using undercompaction. *Geotech. Test. J.* 1 (1), 16–23.
- Li, X.S., Wang, Y., 1998. Linear representation of steady-state line for sand. *J. Geotech. Geoenviron. Eng.* 124 (12), 1215–1217.
- Liang, L., 2016. Static Liquefaction of Sand-Fines Mixtures with the Presence of Initial Shear Stress. The University of Hong Kong, MPhil Thesis.
- Liu, N., Mitchell, J.K., 2006. Influence of nonplastic fines on shear wave velocity-based assessment of liquefaction. *J. Geotech. Geoenviron. Eng.* 132 (8), 1091–1097.
- Murthy, T.G., Loukidis, D., Carraro, J.A.H., Prezzi, M., Salgado, R., 2007. Undrained monotonic response of clean and silty sands. *Géotechnique* 57 (3), 273–288.
- Papadopoulou, A., Tika, T., 2008. The effect of fines on critical state and liquefaction resistance characteristics of non-plastic silty sands. *Soils Found.* 48 (5), 713–725.
- Polito, C.P., 1999. The Effects of Non-Plastic and Plastic Fines on The Liquefaction of Sandy Soils PhD Thesis. Virginia Polytechnic Institute and State University.
- Polito, C.P., Martin, J.R., 2003. A reconciliation of the effects of non-plastic fines on the liquefaction resistance of sands reported in the literature. *Earthq. Spectra* 19 (3), 635–651.
- Seed, H.B., Idriss, I.M., 1982. Ground Motions and Soil Liquefaction During Earthquakes. Earthquake Engineering Research Institute, Oakland, California.
- Shen, C.K., Vrymoed, J.L., Uyeno, C.K., 1977. The effects of fines on liquefaction of sands. In: *Proc. 9th Int. Conf. Soil Mech.* Found. Eng., Tokyo, Japan.
- Stamatopoulos, C.A., 2010. An experimental study of the liquefaction strength of silty sands in terms of the state parameter. *Soil Dyn. Earthq. Eng.* 30 (8), 662–678.
- Stamatopoulos, C.A., Lopez-Caballero, F., Modaressi-Farahmand-Razavi, A., 2015. The effect of preloading on the liquefaction cyclic strength of mixtures of sand and silt. *Soil Dyn. Earthq. Eng.* 78, 189–200.
- Sze, H.Y., 2010. Initial shear and confining stress effects on cyclic behaviour and liquefaction resistance of sands PhD Thesis. The University of Hong Kong.
- Sze, H.Y., Yang, J., 2014. Failure modes of sand in undrained cyclic loading: impact of sample preparation. *J. Geotech. Geoenviron. Eng.* 140 (1), 152–169.
- Thevanayagam, S., Fiorillo, M., Liang, J., 2000. Effect of non-plastic fines on undrained cyclic strength of silty sands. *Soil Dyn. Liq.* 2000, Geo-Denver 2000. Denver, USA
- Thevanayagam, S., Shenthana, T., Mohan, S., Liang, J., 2002. Undrained fragility of clean sands, silty sands, and sandy silts. *J. Geotech. Geoenviron. Eng.* 128 (10), 849–859.
- Wei, L., 2012. Static liquefaction and flow failure of sandy soils PhD Thesis. The University of Hong Kong.
- Wei, X., Guo, Y., Yang, J., Guo, C.B., 2018. Liquefaction characteristics of four Ya-An low-plastic silty sands with presence of initial static shear stress. In: *Proceedings, GeoShanghai 2018*, Shanghai, China.
- Wei, X., Yang, J., Guo, Y., 2017. Investigating the effects of particle shape on liquefaction resistance of sands from critical state perspective. In: *Proc. 6th Int. Young Geotech. Eng. Conf.*, Seoul, Korea.
- Wei, X., Yang, J., 2019. Cyclic behavior and liquefaction resistance of silty sands with presence of initial static shear stress. *Soil Dyn. Earthq. Eng.* 122, 274–289. <https://doi.org/10.1016/j.soildyn.2018.11.029>.
- Xenaki, V.C., Athanasopoulos, G.A., 2003. Liquefaction resistance of sand–silt mixtures: an experimental investigation of the effect of fines. *Soil Dyn. Earthq. Eng.* 23 (3), 1–12.
- Yang, J., 2002a. Non-uniqueness of flow liquefaction line for loose sand. *Geotechnique* 52, 757–760.
- Yang, J., 2002b. Liquefaction resistance of sand in relation to P-wave velocity. *Géotechnique* 52 (4), 295–298.
- Yang, J., Li, X., 2004. State-dependent strength of sands from the perspective of unified modeling. *J. Geotech. Geoenviron. Eng.* 130 (2), 186–198.
- Yang, J., Liu, X., 2016. Shear wave velocity and stiffness of sand: the role of non-plastic fines. *Géotechnique* 66 (6), 500–514.
- Yang, J., Savidis, S., Roemer, M., 2004. Evaluating liquefaction strength of partially saturated sand. *J. Geotech. Geoenviron. Eng.* 130 (9), 975–979.
- Yang, J., Sze, H.Y., 2011a. Cyclic behaviour and resistance of saturated sand under non-symmetrical loading conditions. *Géotechnique* 61 (1), 59–73.
- Yang, J., Sze, H.Y., 2011b. Cyclic strength of sand under sustained shear stress. *J. Geotech. Geoenviron. Eng.* 137 (12), 1275–1285.
- Yang, J., Wei, L.M., 2012. Collapse of loose sand with the addition of fines: the role of particle shape. *Géotechnique* 62 (12), 1111–1125.
- Yang, J., Wei, L.M., Dai, B.B., 2015. State variables for silty sands: Global void ratio or skeleton void ratio?. *Soils Found.* 55 (1), 99–111.
- Yasuda, S., Harada, K., Ishikawa, K., Kanemaru, Y., 2012. Characteristics of liquefaction in Tokyo Bay area by the 2011 Great East Japan Earthquake. *Soils Found.* 52 (5), 793–810.
- Youd, T., Idriss, I., Andrus, R., Arango, I., Castro, G., Christian, J., Dobry, R., Finn, W., Harder, L.J., Hynes, M., Ishihara, K., Koester, J., Liao, S., Marcuson III, W., Martin, G., Mitchell, J., Moriwaki, Y., Power, M., Robertson, P., Seed, R., Stokoe II, K., 2001. Liquefaction resistance of soils: summary report from the 1996 NCEER and 1998 NCEER/NSF workshops on evaluation of liquefaction resistance of soils. *J. Geotech. Geoenviron. Eng.* 127 (10), 817–833.